Wrinkling of a compressed elastic film on a viscous layer

R. Huang[a)]
Department of Civil and Environmental Engineering, Princeton University, Princeton, New Jersey 08544

Z. Suo
*Department of Mechanical and Aerospace Engineering and Princeton Materials Institute,
Princeton University, Princeton, New Jersey 08544*

A compressively strained elastic film bonded to a viscous layer can form wrinkles. The present study provides a theoretical model for the wrinkling process. The elastic film is modeled with the nonlinear theory of a thin plate subject to in-plane and out-of-plane loads. The flow of the viscous layer is modeled with the theory of lubrication. The interface between the elastic film and the viscous layer is assumed to be perfect with no slipping or debonding. A set of partial differential equations evolves the deflection and the in-plane displacements as functions of time. A linear stability analysis identifies the critical wave number, below which the elastic film is unstable and the wrinkles can grow. For any fixed wave number less than the critical wave number, the wrinkles reach a kinetically constrained equilibrium configuration, in which the stress is partially relaxed in the elastic film and the viscous layer stops flowing. Numerical simulations reveal rich dynamics of the system with many unstable equilibrium configurations. © *2002 American Institute of Physics.*
[DOI: 10.1063/1.1427407]

I. INTRODUCTION

Various types of compliant substrates have been fabricated to grow relaxed heteroepitaxial films with low dislocation density for optoelectronic applications.[1] In the recent experiments by Hobart *et al.*,[2] a strain-relaxed substrates was formed by transferring a compressively strained heteroepitaxial SiGe film to a Si substrate covered with a glass layer through wafer bonding. Upon annealing above the glass transition temperature, the SiGe film formed wrinkles at the center of the film, but extended at the edges. Figure 1 schematically shows the flat and the wrinkled states of an elastic film on a viscous layer, which in turn lies on a rigid substrate. Similar wrinkling pattern has also been observed in other systems, such as thermally grown oxides on metals[3–5] and thin metal films on polymers.[6,7] While the compliant substrate technology for optoelectronic applications usually requires the films to be flat with no wrinkles, the formation and control of the ordered pattern may find uses in optical devices as diffraction gratings and microfluidic devices in making channels with microstructured walls.[7]

Previous studies on stress relaxation of an elastic film on a viscous layer tend to separate deflection and in-plane extension. Freund and Nix[8] considered the in-plane extension using the shear lag model, and Sridhar *et al.*[9] studied the kinetics of wrinkling with only the deflection. However, deflection and in-plane extension are inherently coupled, because the flow conserves the volume of the viscous layer, and the deflection relaxes the compressive stress in the elastic film. In the present study, the flow in the viscous layer is approximated by the theory of lubrication.[10] The elastic film

is modeled as a thin plate under the combined action of in-plane and out-of-plane loads. To allow large deflection, the nonlinear Von Karman plate theory[11,12] is applied with a minor change to include the shear stresses at the interface.

The plan for the article is as follows. Section II formulates the problem and reduces the formulations under the plane strain conditions. A linear stability analysis is performed in Sec. III to determine the critical wave number of wrinkling. For any fixed wave number less than the critical wave number, the solution for the kinetically constrained equilibrium state is obtained in Sec. IV. Numerical simulations in Sec. V show rich dynamics of the wrinkling process.

II. COUPLED VISCOUS FLOW AND ELASTIC DEFORMATION

To formulate the problem, we describe the viscous layer with the lubrication theory, and the elastic film with the nonlinear thin plate theory. The viscous layer and the elastic film are coupled at the interface, where the traction vector and the velocity vector are continuous. The formulation is for three-dimensional flow and deformation, but is reduced to the plane strain field at the end, which will be applied in the remaining sections.

A. Flow of the viscous layer

Since the thickness of the viscous layer is small compared with the characteristic lengths in the *x* and *y* directions, such as the wavelength of the wrinkles, we describe the viscous layer using the theory of lubrication.[10] Such approximation has been used to model the surface evolution in thin liquid films, describing the three-dimensional flow with two-dimensional partial differential equations.[13,14] In the lubrication theory, the Navier–Stokes equations for incompressible viscous flow reduce to

---

[a)]Author to whom correspondence should be addressed; electronic mail: ruihuang@princeton.edu
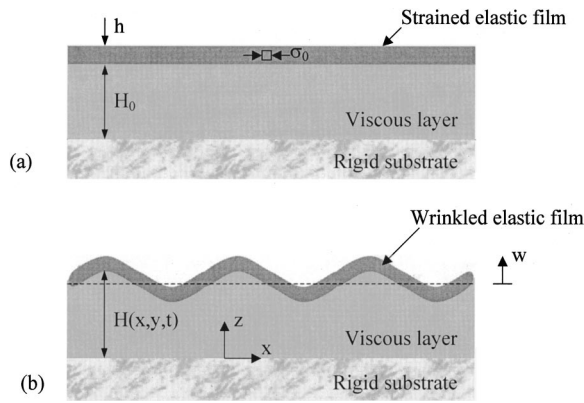
1135

FIG. 1. Schematic illustration of a compressed elastic film on a viscous layer. (a) The trivial equilibrium state where the film is flat and biaxially stressed. (b) A wrinkled state.

$$\frac{\partial^2 v_\alpha}{\partial z^2} = \frac{1}{\eta} \frac{\partial p}{\partial x_\alpha}, \tag{1}$$

where η is the viscosity and p is the pressure. The greek suffix α takes the two values x and y, and v_x, v_y are the flow velocities in the x and y directions. The shear stresses arising from the viscosity are

$$\tau_{z\alpha} = \eta \frac{\partial v_\alpha}{\partial z}. \tag{2}$$

The no-slip boundary condition is assumed at the bottom of the viscous layer, i.e., $v_x = v_y = 0$ at $z = 0$. Let $H(x,y,t)$ be the varying thickness of the viscous layer. At the top of the viscous layer, $z = H(x,y,t)$, we prescribe shear stresses: $\tau_{zx} = T_x$ and $\tau_{zy} = T_y$. The pressure p is independent of z in the theory of lubrication, such that Eq. (1) can be integrated twice with respect to z, giving

$$v_\alpha = \frac{1}{2\eta} \frac{\partial p}{\partial x_\alpha} z(z - 2H) + \frac{T_\alpha}{\eta} z. \tag{3}$$

The flow rates in the x and y directions are

$$Q_\alpha = \int_0^H v_\alpha \, dz = -\frac{H^3}{3\eta} \frac{\partial p}{\partial x_\alpha} + \frac{H^2}{2\eta} T_\alpha, \tag{4}$$

and the mass conservation requires that

$$\frac{\partial H}{\partial t} + \frac{\partial Q_\alpha}{\partial x_\alpha} = 0. \tag{5}$$

Let u_x and u_y be the displacements at the top surface of the viscous layer in the x and y directions, and w be the displacement in the z directions. Let H_0 be the initial thickness of the viscous layer, so that $H(x,y,t) = H_0 + w(x,y,t)$. Equations (5) and (3) give

$$\frac{\partial w}{\partial t} = \frac{\partial}{\partial x_\alpha} \left(\frac{H^3}{3\eta} \frac{\partial p}{\partial x_\alpha} - \frac{H^2}{2\eta} T_\alpha \right), \tag{6}$$

$$\frac{\partial u_\alpha}{\partial t} = -\frac{H^2}{2\eta} \frac{\partial p}{\partial x_\alpha} + \frac{H}{\eta} T_\alpha. \tag{7}$$

Equations (6) and (7) evolve the displacements once we relate the tractions p and T_α to the displacement field. These relations will be provided by analyzing the elastic deformation of the thin film in the next subsection.

B. Deformation of the elastic film

We now turn our attention to the elastic film. The nonlinear theory[11,12] for large deflections of thin elastic plates under in-plane and out-of-plane loads is employed for the film. The elastic film is bonded to the viscous layer, so that the displacements and tractions are continuous across the interface. That is, the elastic film is subject to the pressure p and the shear stresses T_x and T_y, and the displacement components of the film are u_x, u_y, and w. We take the flat, biaxially strained film as the reference state, in which the membrane strain is ε_0 in both x and y directions. The displacements are set to be zero in the reference state. The membrane strains relate to the displacements as

$$\varepsilon_{\alpha\beta} = \varepsilon_0 \delta_{\alpha\beta} + \frac{1}{2} \left(\frac{\partial u_\alpha}{\partial x_\beta} + \frac{\partial u_\beta}{\partial x_\alpha} \right) + \frac{1}{2} \frac{\partial w}{\partial x_\alpha} \frac{\partial w}{\partial x_\beta}. \tag{8}$$

The nonlinear plate theory includes the term quadratic in the slope of the deflection.

Hooke's law relates the membrane forces in the film to the membrane strains, namely,

$$N_{\alpha\beta} = Eh \left[\frac{1}{1+\nu} \varepsilon_{\alpha\beta} + \frac{\nu}{1-\nu^2} \varepsilon_{\gamma\gamma} \delta_{\alpha\beta} \right], \tag{9}$$

where E is Young's modulus, ν is Poisson's ratio, and h is the thickness of the film. In the reference state, $N_{xx} = N_{yy} = \sigma_0 h$ and $N_{xy} = 0$, where $\sigma_0 = E\varepsilon_0/(1-v)$ is the biaxial stress when the film is flat.

Equilibrium in the plane of the film requires that

$$T_\alpha = \frac{\partial N_{\alpha\beta}}{\partial x_\beta}. \tag{10}$$

Equilibrium in the direction perpendicular to the plane and equilibrium of moments require that

$$p = D \frac{\partial^4 w}{\partial x_\alpha \partial x_\alpha \partial x_\beta \partial x_\beta} - N_{\alpha\beta} \frac{\partial^2 w}{\partial x_\alpha \partial x_\beta} - T_\alpha \frac{\partial w}{\partial x_\alpha}, \tag{11}$$

where D is the flexural rigidity of the elastic film, i.e., $D = [Eh^3/12(1-\nu^2)]$.

Equations (8)–(11) relate the tractions, p and T_α, to the displacements, w and u_α. These relations, together with Eqs. (6) and (7), form a complete system governing the relaxation process of a strained elastic film on a viscous layer.

The elastic strain energy stored in the film provides the driving force of the relaxation process. The strain energy arises from two processes: bending and in-plane deformation. The energy density (energy per unit area) due to bending is

$$\Phi_1 = \frac{D}{2}\left[\left(\frac{\partial^2 w}{\partial x^2} + \frac{\partial^2 w}{\partial y^2}\right)^2 - 2(1-\nu)\right.$$
$$\left.\times\left(\frac{\partial^2 w}{\partial x^2}\frac{\partial^2 w}{\partial y^2} - \left(\frac{\partial^2 w}{\partial x\partial y}\right)^2\right)\right]. \tag{12}$$

The energy density due to in-plane deformation is

$$\Phi_2 = \frac{1}{2}N_{\alpha\beta}\varepsilon_{\alpha\beta}. \tag{13}$$

The total elastic energy density in the film is $\Phi = \Phi_1 + \Phi_2$.

C. Reduced formulations under the plane strain conditions

Since the film is initially strained in both the x and y directions, relaxation occurs simultaneously in both directions. To make the problem simpler, the remainder of this paper assumes that relaxation occurs only in the x direction, such that the deformation is in a state of plane strain, i.e., $u_x = u_x(x,t)$, $w = w(x,t)$, and $u_y = 0$. Thus, the evolution equations (6) and (7) reduce to

$$\frac{\partial w}{\partial t} = \frac{\partial}{\partial x}\left(\frac{H^3}{3\eta}\frac{\partial p}{\partial x} - \frac{H^2}{2\eta}T_x\right), \tag{14}$$

$$\frac{\partial u_x}{\partial t} = -\frac{H^2}{2\eta}\frac{\partial p}{\partial x} + \frac{H}{\eta}T_x. \tag{15}$$

The shear stress T_x and the pressure p are

$$T_x = \frac{\partial N_{xx}}{\partial x}, \tag{16}$$

$$p = D\frac{\partial^4 w}{\partial x^4} - N_{xx}\frac{\partial^2 w}{\partial x^2} - T_x\frac{\partial w}{\partial x}. \tag{17}$$

The membrane forces are

$$N_{xx} = \sigma_0 h + \frac{Eh}{1-\nu^2}\left[\frac{\partial u_x}{\partial x} + \frac{1}{2}\left(\frac{\partial w}{\partial x}\right)^2\right], \tag{18}$$

$$N_{yy} = \sigma_0 h + \frac{\nu Eh}{1-\nu^2}\left[\frac{\partial u_x}{\partial x} + \frac{1}{2}\left(\frac{\partial w}{\partial x}\right)^2\right], \tag{19}$$

and $N_{xy} = 0$. The membrane strain components are

$$\varepsilon_{xx} = \varepsilon_0 + \frac{\partial u_x}{\partial x} + \frac{1}{2}\left(\frac{\partial w}{\partial x}\right)^2, \quad \varepsilon_{yy} = \varepsilon_0, \quad \varepsilon_{xy} = 0. \tag{20}$$

The energy densities in Eqs. (12) and (13) reduce to

$$\Phi_1 = \frac{D}{2}\left(\frac{\partial^2 w}{\partial x^2}\right)^2, \tag{21}$$

$$\Phi_2 = \frac{1}{2}(N_{xx}\varepsilon_{xx} + N_{yy}\varepsilon_{yy}). \tag{22}$$

III. LINEAR PERTURBATION ANALYSIS

The remainder of this article considers a compressively strained infinite film under the plane strain conditions. That is, the lateral dimension of the film is much larger than the wrinkle wavelength, so that the relaxation at the edges of the film is neglected. A flat film with the uniform biaxial strain ε_0 and stress $\sigma_0 = E\varepsilon_0/(1-\nu)$ is a trivial equilibrium state, in which $w = u_x = 0$, $N_{xx} = N_{yy} = \sigma_0 h$, and $p = T_x = 0$, as shown in Fig. 1(a). The total elastic energy density is $\Phi = \sigma_0\varepsilon_0 h$. In this state, according to Eqs. (14) and (15), $\partial w/\partial t = \partial u_x/\partial t = 0$. Consequently, the film does not evolve. However, this equilibrium state is unstable. The elastic energy reduces when the film forms wrinkles.

Perturb the displacements as

$$w(x,t) = A(t)\sin(kx), \tag{23}$$

$$u(x,t) = B(t)\cos(kx), \tag{24}$$

where A and B are small amplitudes. Substituting Eqs. (23) and (24) into Eqs. (18), (16), and (17), and keeping only the first order terms in A and B, we obtain that

$$N_{xx} = \sigma_0 h - \frac{Ehk}{1-\nu^2}B\sin(kx), \tag{25}$$

$$T_x = -\frac{Ehk^2}{1-\nu^2}B\cos(kx), \tag{26}$$

$$p = \left[\sigma_0 hk^2 + \frac{Ek^4 h^3}{12(1-\nu^2)}\right]A\sin(kx). \tag{27}$$

Inserting Eqs. (26) and (27) into Eqs. (14) and (15), we obtain that

$$\frac{dA}{dt} = \alpha A - \frac{1}{2}\beta k H_0 B, \tag{28}$$

$$\frac{dB}{dt} = \frac{3\alpha}{2kH_0}A - \beta B, \tag{29}$$

where

$$\alpha = \frac{E(kH_0)^3}{36\eta(1-\nu^2)}[-12\varepsilon_0(1+\nu)(kh) - (kh)^3], \tag{30}$$

$$\beta = \frac{E(kh)(kH_0)}{\eta(1-\nu^2)}. \tag{31}$$

Equations (28) and (29) are two coupled linear ordinary differential equations. The solution takes the form

$$A(t) = A_1\exp(s_1 t) + A_2\exp(s_2 t), \tag{32}$$

$$B(t) = B_1\exp(s_1 t) + B_2\exp(s_2 t), \tag{33}$$

where

$$s_1 = \tfrac{1}{2}[(\alpha-\beta) + \sqrt{(\alpha-\beta)^2 + \alpha\beta}], \tag{34}$$

$$s_2 = \tfrac{1}{2}[(\alpha-\beta) + \sqrt{(\alpha-\beta)^2 + \alpha\beta}], \tag{35}$$

and

$$\frac{B_1}{A_1} = \frac{2(\alpha-s_1)}{\beta kH_0}, \quad \frac{B_2}{A_2} = \frac{2(\alpha-s_2)}{\beta kH_0}. \tag{36}$$

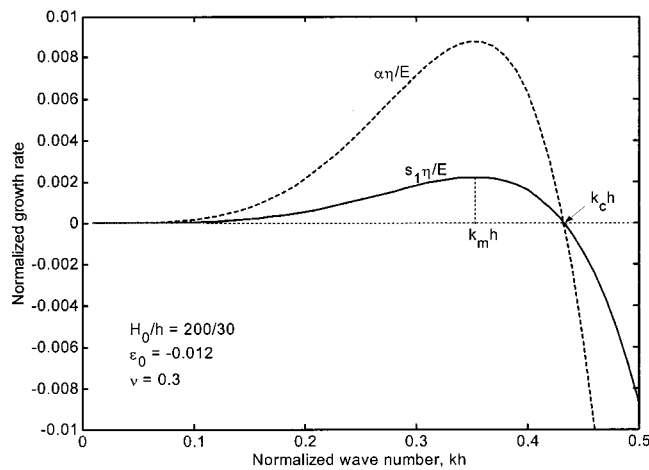Let the initial amplitudes be $A(0) = A_0$ and $B(0) = B_0$, so that

FIG. 2. The normalized growth rate as a function of the normalized wave number.

FIG. 3. The normalized critical wave number and the fastest growing wave number as functions of the initial compressive strain.

$$A_1 = \frac{\alpha - s_2}{s_1 - s_2} A_0 - \frac{\beta k H_0}{2(s_1 - s_2)} B_0, \tag{37}$$

$$A_2 = \frac{\alpha - s_1}{s_2 - s_1} A_0 - \frac{\beta k H_0}{2(s_2 - s_1)} B_0, \tag{38}$$

and B_1, B_2 can be obtained from Eq. (36).

For any given wave number k, $\beta > 0$ and $s_2 < 0$. Consequently, the s_2 mode in Eqs. (32) and (33) always decays exponentially with time. For the s_1 mode, however, there exists a critical wave number

$$k_c h = \sqrt{-12\varepsilon_0(1+\nu)}. \tag{39}$$

When $k > k_c$, $\alpha < 0$ and $s_1 < 0$, so that the perturbations decay and the trivial equilibrium state is stable. When $k < k_c$, $\alpha > 0$ and $s_1 > 0$, so that the perturbation grows exponentially and the trivial equilibrium state is unstable. The critical wave number is an outcome of the trade-off between bending and in-plane deformation. The film wrinkles to reduce the elastic energy due to the compressive in-plane deformation. Upon wrinkling, the film acquires some bending energy. The bending energy is low when the wave number is small. The stability condition is identical to that of Euler buckling, and α is the same as the growth rate of buckling amplitude in Ref. 7 in the limit of small thickness of the viscous layer. However, the growth rate from the present analysis is s_1, which is different from α. For comparison, Fig. 2 shows the growth rate as a function of the wave number for given initial strain $\varepsilon_0 = -0.012$, thickness ratio $H_0/h = 200/30$, and Poisson's ratio $\nu = 0.3$. The solid line is the growth rate and the dashed line is α. When $kh \to 0$, the wrinkles have long waves, and it takes a long time for the viscous material under the film to flow to accommodate the wrinkling process, so that the growth rate is small. When $kh \to \infty$, the wrinkles have short waves, and the bending energy is too high to trade off with the in-plane elastic energy, so that wrinkles decay. The growth rate becomes positive when $k < k_c$, and reaches a peak at a wave number k_m.

The difference between the present analysis and the analysis in Ref. 7 is that, in the present analysis, the in-plane displacement is not zero, neither is the shear stress at the
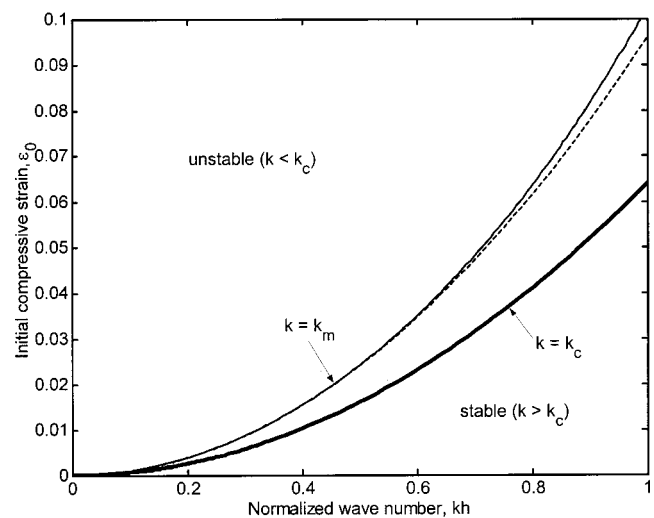
interface. This is because the pressure at the surface of the viscous layer is not uniformly distributed and thus forces the viscous flow parallel to the surface. While in Ref. 7, the shear stress at the interface is neglected.

The fastest growing wave number, k_m, can be found by setting $\partial s_1/\partial k = 0$, as shown by the thin solid line in Fig. 3. The dashed line in Fig. 3 is from the linear stability analysis in Ref. 7 in the limit of small viscous layer thickness. Although the present study gives a different growth rate of the wrinkling, the fastest growing wave number is close to the previous study. It is also found that the fastest growing wave number from the present study slightly depends on the thickness ratio between the viscous layer and the elastic film. The thick solid line in Fig. 3 shows the critical wave number.

In the experiments of Hobart et al.,[2] they found the wavelength of the wrinkles is approximately 1 μm for a film with $\varepsilon_0 = 0.012$, $h = 30$ nm, and $H_0 = 200$ nm. Assuming that this corresponds to the fastest growing wavelength (λ_m
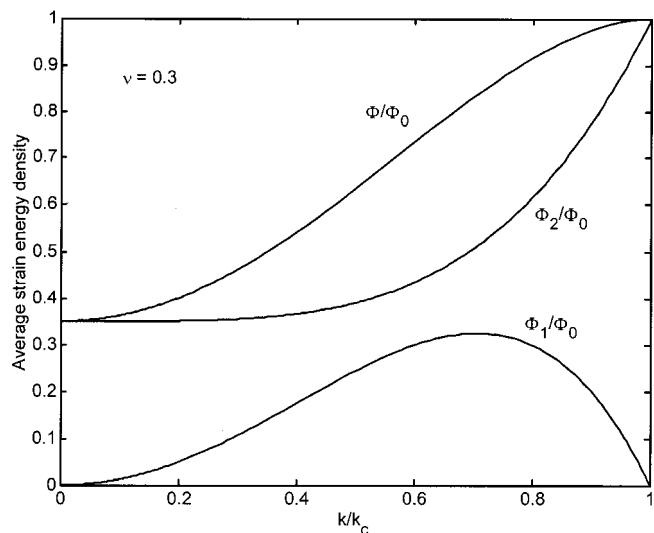

FIG. 4. The average strain energy densities of the kinetically constrained equilibrium wrinkles as functions of the wave number.
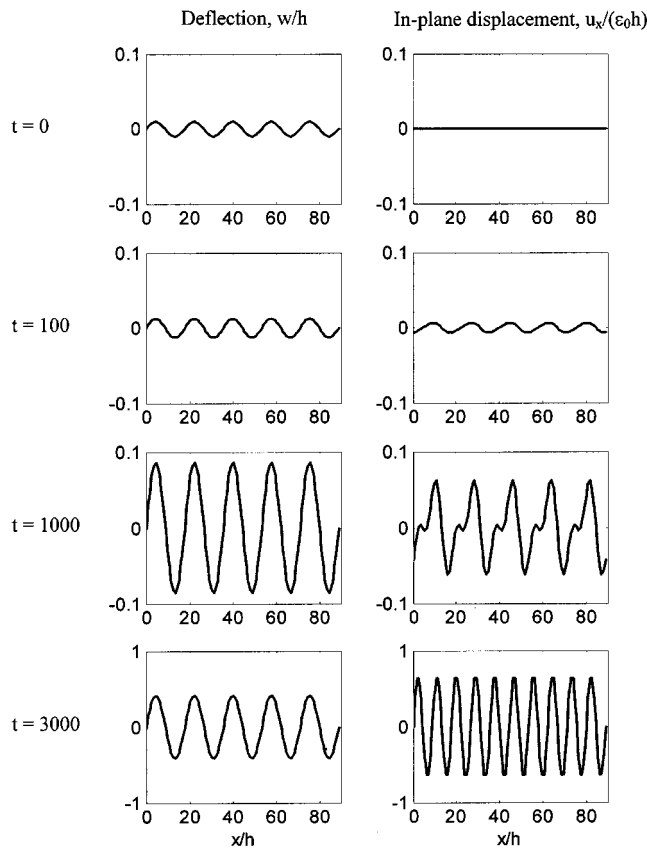
FIG. 5. Distributions of the normalized deflection and in-plane displacement at different times from the numerical simulation with the wave number $kh = 0.3533$.
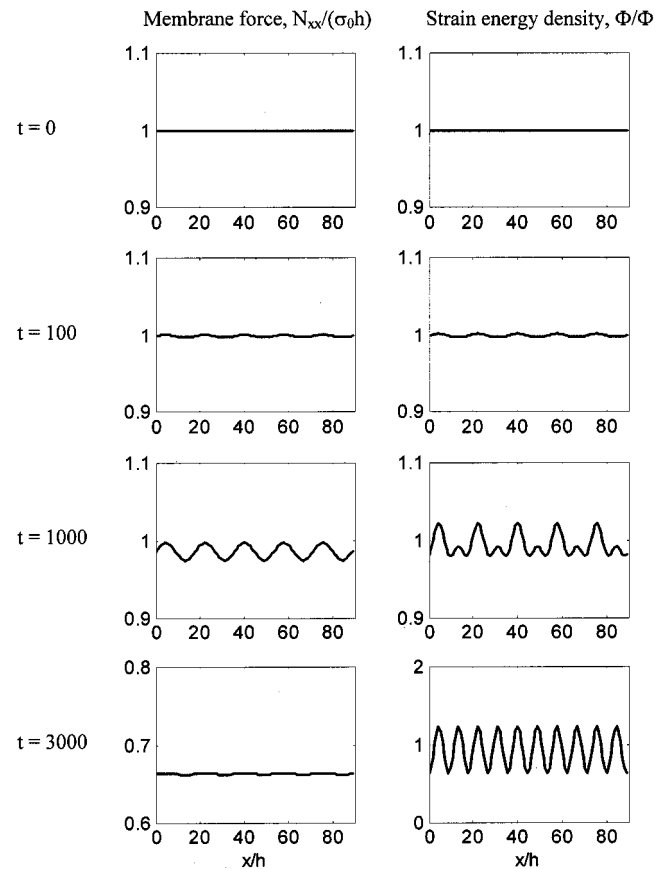

FIG. 6. Distributions of the normalized membrane force and strain energy density at different times from the numerical simulation with the wave number $kh = 0.3533$.

$= 2\pi/k_m$), the present analysis predicts a wavelength of 0.53 μm, which is in reasonable agreement with the experiments (i.e., less than a factor of 2).

IV. KINETICALLY CONSTRAINED EQUILIBRIUM WRINKLES

When an elastic column in the air is subject to a large enough axial compression at two ends, the column buckles to an equilibrium configuration. Depending on the type of constraint at the ends, the equilibrium configuration takes the shape of a half or a whole period of a sinusoidal curve. Equilibrium configurations with shorter waves do exist. However, these configurations are of higher energy than the fundamental mode. The column in the air can quickly settle to the fundamental mode.

For a large area elastic film on a viscous layer, experiments have shown that the film can stay in the state of short wave wrinkles for a long time.[2,15] Indeed, for any wave number $k < k_c$, there is an equilibrium wrinkle state. Once the film is in the neighborhood of such an equilibrium state, the viscosity of the underlayer makes the film stay there for a long time before the film further evolves to lower energy, longer wave wrinkles. That is, all these equilibrium states are unstable, but the film may spend a long time in such a state simply because of the kinetic constraint of the viscous layer.

The film reaches the unstable equilibrium states when the viscous layer stops flowing and the tractions at the inter-

face vanish, i.e., $p = T_x = 0$. Consequently, Eq. (16) requires that N_{xx} be independent of x, and Eq. (17) becomes

$$D \frac{\partial^4 w}{\partial x^4} = N_{xx} \frac{\partial^2 w}{\partial x^2}. \tag{40}$$

Let k be a given wave number of the equilibrium wrinkle. Equation (40) has a solution in the form

$$w = A_{eq} \sin(kx), \tag{41}$$

where the equilibrium wrinkle amplitude, A_{eq}, is to be determined as a function of the wrinkle wave number. Substituting Eq. (41) into Eq. (40), we obtain that

$$N_{xx} = \left(\frac{k}{k_c}\right)^2 \sigma_0 h, \tag{42}$$

where k_c is given by Eq. (39). As anticipated, the longer the wrinkle wave, the smaller the magnitude of the membrane force. The stress is relaxed when $k < k_c$. From Eqs. (18) and (41), we obtain that

$$u_x = -\frac{1}{8} k A_{eq}^2 \sin(2kx). \tag{43}$$

Observe that, in the equilibrium state, the in-plane displacement undulates with the wave number twice the wave number of the deflection.
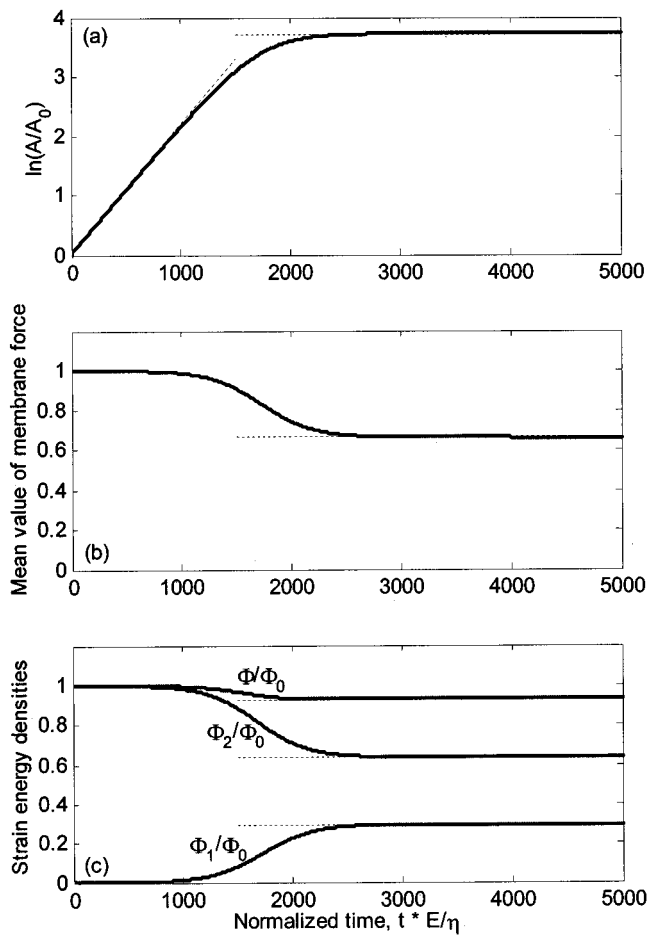
FIG. 7. (a) The amplitude of the wrinkles as a function of time; (b) the average membrane force as a function of time; (c) the average strain energy densities as functions of time.
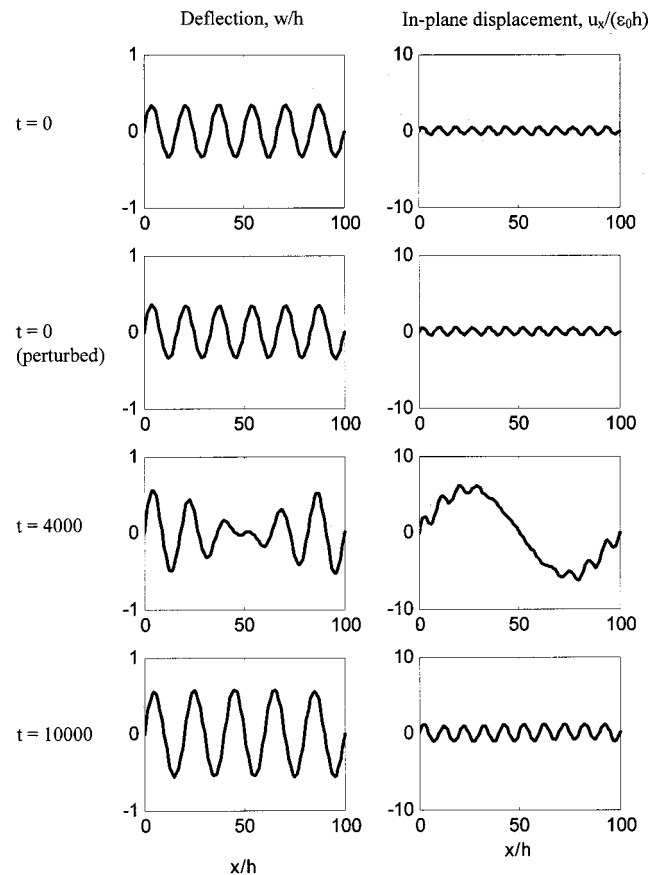

FIG. 8. Distributions of the normalized deflection and in-plane displacement at different times from the numerical simulation with a perturbed deflection from the kinetically constrained equilibrium wrinkles as the initial condition.

Inserting Eqs. (41), (42), and (43) into Eq. (18), we obtain that

$$A_{eq} = h \sqrt{\frac{1}{3}\left[\left(\frac{k_c}{k}\right)^2 - 1\right]}. \tag{44}$$

For $k < k_c$, Eq. (44) gives a real equilibrium amplitude of the wrinkle and the amplitude increases as the wave number decreases. For $k > k_c$, however, A_{eq} is imaginary and the equilibrium state does not exist.

The elastic strain energy densities in the equilibrium states are

$$\Phi_1 = (1+\nu)\Phi_0 \frac{k^2}{k_c^2}\left(1 - \frac{k^2}{k_c^2}\right)[1 - \cos(2kx)], \tag{45}$$

$$\Phi_2 = \frac{\Phi_0}{2}\left[1 - \nu + (1+\nu)\frac{k^4}{k_c^4}\right], \tag{46}$$

where $\Phi_0 = \sigma_0 \varepsilon_0 h$ is the strain energy density in the trivial equilibrium state. The average of the total strain energy density is

$$\Phi = \Phi_0\left[1 - \frac{1+\nu}{2}\left(1 - \frac{k^2}{k_c^2}\right)^2\right]. \tag{47}$$

The total elastic energy is lower at the equilibrium states with a lower wave number. As $k \to 0$, $N_{xx} \to 0$ and $\Phi \to E\varepsilon_0^2 h/2$, which corresponds to the state when the film is fully relaxed in the x direction but under uniaxial compression in the y direction. Figure 4 shows the average energy densities at the equilibrium state as functions of the wave number.

V. NUMERICAL SIMULATIONS

In this section, we solve the nonlinear partial differential equations by using the finite difference method. The forward-time-centered-space (FTCS) differencing scheme is used and the periodic boundary conditions are assumed. The equations are normalized for numerical simulations. In the following discussions, the unit of time is η/E. Using the typical values of $\eta (\sim 10^{10} \text{ N s/m}^2)$ and $E (\sim 10^{11} \text{ N/m}^2)$, an estimate of the time unit is 0.1 second.

A. Sinusoidal deflection as the initial condition

We start the numerical simulation with the initial condition $w(x, t=0) = A_0 \sin(kx)$ and $u(x, t=0) = 0$. Figure 5 shows the distribution of the displacements at different times, and Fig. 6 shows the distributions of the membrane force and the strain energy density. At $t = 0$, the compressive membrane force is slightly relaxed due to the initial deflection. Numerical simulations with various wave numbers of
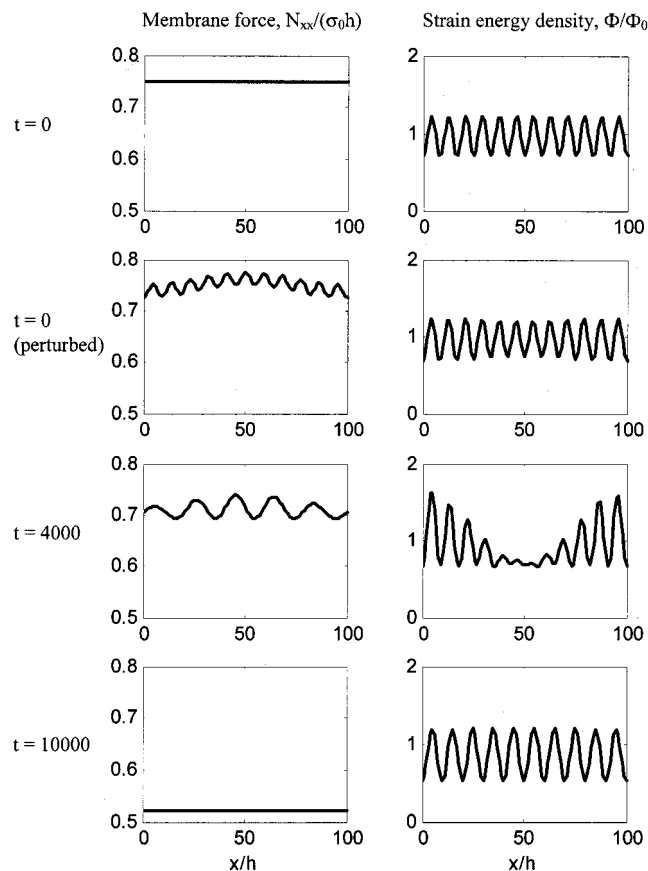
FIG. 9. Distributions of the normalized membrane force and strain energy density at different times from the numerical simulation with a perturbed deflection from the kinetically constrained equilibrium wrinkles as the initial condition.
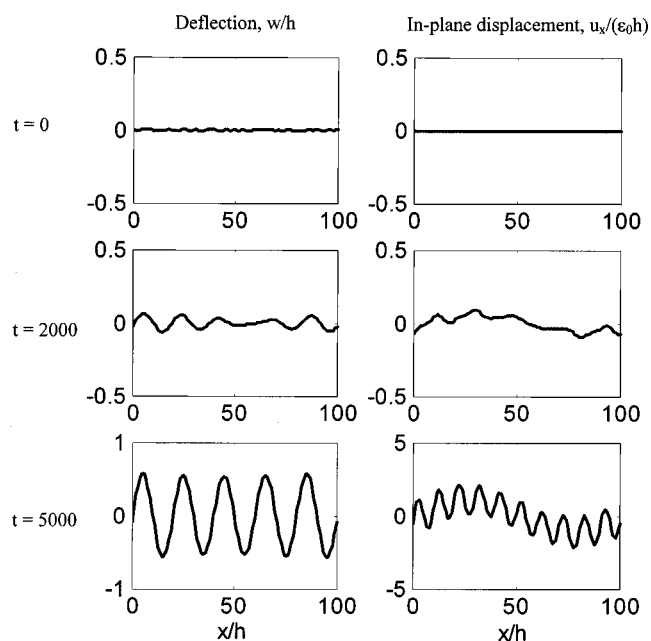

FIG. 10. Distributions of the normalized deflection and in-plane displacement at different times from the numerical simulation with a random deflection as the initial condition.

brane force decreases and reaches the equilibrium value, which is given by Eq. (42) and indicated by the dashed line. Figure 7(c) shows the average strain energy densities as functions of time. As the wrinkle grows, the strain energy due to in-plane deformation decreases, but the strain energy due to bending increases. The total strain energy decreases and reaches the equilibrium value.

the initial deflection confirm that the amplitude of perturbation decays when $k > k_c$ and grows when $k < k_c$, as predicted by the linear perturbation analysis. When the amplitude does grow, the numerical simulation goes beyond the linear perturbation analysis and reaches the kinetically constrained equilibrium state. At the early stage, as in the linear perturbation analysis, the wave number of the in-plane displacement is the same as the deflection. At a later stage, the film tries to reach the constrained equilibrium state, in which the wave number of the in-plane displacement is twice the wave number of deflection. As shown for $t = 1000$, the wave number of the in-plane displacement starts to change. By the time $t = 3000$, the wave number is about twice the initial wave number. Meanwhile, the average value of the membrane force and strain energy density decrease and the distribution of the membrane force is nearly uniform at $t = 3000$. During the entire simulation, the wave number of the deflection remains the same, but its amplitude grows and reaches the equilibrium value. Figure 7(a) shows the wrinkle amplitude as a function of time. At the early stage, the amplitude grows exponentially with the growth rate given by Eq. (32), as shown by the dashed straight line. The dashed horizontal line indicates the equilibrium value of the amplitude, given by Eq. (44). The numerical simulation shows that the amplitude reaches the equilibrium value with less than 2% numerical error. Figure 7(b) shows that the mean value of the mem-
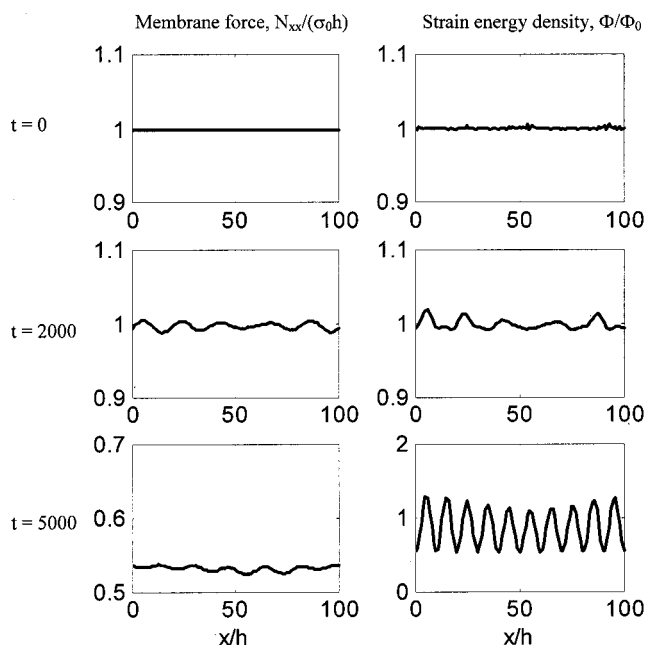

FIG. 11. Distributions of the normalized membrane force and strain energy density at different times from the numerical simulation with a random deflection as the initial condition.

B. Perturbed deflection from the constrained equilibrium state as the initial condition

In the previous numerical simulation, the kinetically constrained equilibrium state is reached and the evolution stops. However, as we mentioned before, the equilibrium is unstable and the strain energy in the elastic film can be further reduced by decreasing the wave number of the wrinkles. To demonstrate the instability of the equilibrium state, we add to the deflection in the equilibrium state with a small amplitude perturbation of a smaller wave number. Figure 8 shows the evolution of the displacement field. The first row shows the displacements in the constrained equilibrium state, which are computed from Eqs. (41) and (43) for $kh = 0.377$. The second row shows the perturbed displacements. The amplitude of the perturbation is small compared to the wrinkle amplitude in the equilibrium state and the wave number is 0.314. Numerical simulation shows that the perturbation grows. At $t = 4000$, as shown in the third row of Fig. 8, the film forms mixed-mode wrinkles. At $t = 10\,000$, the wrinkles reach another equilibrium state with a smaller wave number. Figure 9 shows the evolution of the membrane force and the strain energy density. Both the membrane force and the average strain energy density are reduced in the second equilibrium state.

C. Random deflection as the initial condition

Our third simulation starts with a randomly generated distribution of the initial deflection. Figure 10 shows the evolution of the displacements and Fig. 11 shows the membrane force and the strain energy density. First, all the modes with the wave number less than the critical wave number grow, but the mode with the fastest growth rate dominates. In this particular example, there are two fastest growing modes with nearly the same growth rate. At $t = 2000$, the two modes are mixed. At $t = 5000$, however, the mode with a smaller wave number and lower elastic energy dominates and approaches the equilibrium. As shown in Fig. 2, for $k < k_m$, the growth rate decreases as k decreases. Therefore, further relaxation to the modes with even smaller wave numbers becomes increasingly slower. This explains why the film can stay in a wrinkling state with the fastest growing wave number for a long time.

VI. CONCLUDING REMARKS

A compressively strained elastic film on a viscous layer forms wrinkles. We formulate a set of nonlinear partial differential equations to evolve the shape. The elastic film is modeled by the nonlinear thin-plate theory, and the viscous layer by the theory of lubrication. Wrinkling is a compromise between elastic energy as a driving force, and the viscous flow as a kinetic process. If the waves are too short, the bending costs too much elastic energy, and the wrinkles decay. If the waves are too long, the viscous flow takes too much time for the shape to change noticeably. The wrinkles have infinitely many unstable equilibrium configurations. The longer the wave, the lower the elastic energy. However, these unstable wrinkles are kinetically constrained. The elastic film may spend a long time in the neighborhood of one equilibrium configuration before evolving further into a longer wave to lower the elastic energy. Our numerical simulations start with the perturbations of the flat film and the unstable wrinkles, and reveal rich dynamics of the wrinkling process. The complex energy landscape merits further investigations.

[1] K. Vanhollebeke, I. Moerman, P. Van Daele, and P. Demeester, Prog. Cryst. Growth Charact. Mater. **41**, 1 (2000).
[2] K. D. Hobart, F. J. Kub, M. Fatemi, M. E. Twigg, P. E. Thompson, T. S. Kuan, and C. K. Inoki, J. Electron. Mater. **29**, 897 (2000).
[3] Z. Suo, J. Mech. Phys. Solids **43**, 829 (1995).
[4] V. K. Tolpygo and D. R. Clarke, Acta Mater. **46**, 5153 (1998).
[5] V. K. Tolpygo and D. R. Clarke, Acta Mater. **46**, 5167 (1998).
[6] N. Bowden, S. Brittain, A. G. Evans, J. W. Hutchinson, and G. M. Whitesides, Nature (London) **393**, 146 (1998).
[7] W. T. S. Huck, N. Bowden, P. Onck, T. Pardoen, J. W. Hutchinson, and G. M. Whitesides, Langmuir **16**, 3497 (2000).
[8] L. B. Freund and W. D. Nix (unpublished).
[9] N. Sridhar, D. J. Srolovitz, and Z. Suo, Appl. Phys. Lett. **78**, 2482 (2001).
[10] O. Reynolds, Philos. Trans. R. Soc. London **177**, 157 (1886).
[11] S. Timoshenko and S. Woinowsky-Krieger, *Theory of Plates and Shells*, 2nd ed. (McGraw-Hill, New York, 1987).
[12] L. D. Landau and E. M. Lifshitz, *Theory of Elasticity* (Pergamon, London, 1959), pp. 57–60.
[13] M. B. Williams and S. H. Davis, J. Colloid Interface Sci. **90**, 220 (1982).
[14] E. Ruckenstein and R. K. Jain, J. Chem. Soc., Faraday Trans. 2 **70**, 132 (1974).
[15] H. Yin, J. C. Sturm, Z. Suo, R. Huang, and K. D. Hobart, presented at the 43rd Electronic Materials Conference, Notre Dame, Indiana, June 2001.